IJCRT.ORG ISSN : 2320-2882

INTERNATIONAL JOURNAL OF CREATIVE RESEARCH THOUGHTS (IJCRT)

An International Open Access, Peer-reviewed, Refereed Journal

Three-Port Converter with Grid Connected system for Hybrid Power Distributed and Generation System

K. Pratap[1],K. Rambabu[2],CH. Amarendra[3]

M.Tech student[1],Associate Professor[2],[3]Associate Professor

Department of Electrical and Electronics Engineering,

[1]Aditya Engineering College(A), Surampalem, Andhra Pradesh, India

Abstract:Environmental constraints and the limited supply of fuel make conventional power production methods susceptible. The current electrical power system is developing toward distributed generation, which provides several advantages to the market participants. Recent days have seen a surge in interest in hybrid distributed power-producing devices that combine battery storage with renewable energy sources. There are two converters in conventional systems, one for PV and one for the battery. It is proposed in this research that a PV/battery hybrid distributed power generating system with just one integrated 3-port power converter employs an energy management and control technique. To achieve a balance of power throughout three ports in various operating situations, a method for energy management and control is provided that takes into account both maximum power point tracking (MPPT) and battery charging/discharging management. MATLAB /Simulink is used to examine the simulation model and its output.

Index Terms **– MPPT, PV System, Battery Management.**

I. INTRODUCTION

Rapid fossil fuel depletion and global warming have required an urgent need for alternative energy to meet the ever-increasing energy demand. Renewable energy is becoming more important because of the adverse effects on the environment and the high expense of conventional power plants. Greenhouse gas emissions are a consequence of the usage of fossil fuels in power plants. Because of the rising global population and the resulting rise in energy demand, these greenhouse gas emissions are having an increasingly negative impact on the environment. Hybrid power systems have had to evolve as a result of the scarcity of traditional fossil fuel supplies. As a result, adding RES to the system offers additional opportunities for balancing the system's load demand. Reducing dependence on fossil fuels while maintaining supply and demand balance is possible with a hybrid energy system. Hybrid power systems provide high levels of operating efficiency and dependability [1,18]. It is possible to overcome the constraints of wind and solar resources by using a hybrid power system since their performance characteristics are affected by adverse climatic circumstances. As a general rule, hybrid stand-alone electricity production systems tend to be more dependable and less expensive than systems that rely on a single source of energy. One environmental factor, on the other hand, may make one RES technology more lucrative than another.Photovoltaic (PV) systems are good for areas with a lot of sunlight, whereas Wind power systems are ideal for areas with strong winds [4].

Solar and wind power systems are combined in this way: the PV system is made up of solar panels, a maximum power point tracking (MPPT) boost converter, and an MPPT boost converter for the wind turbines (SWHPS). The MPPT boost converter's control technique has a major impact on the SWHPS's efficiency and dependability. Without adequate control logic in the MPPT boost converter, solar and wind power production cannot run at maximum power point (MPP). Even when wind and solar power are available, the output voltage of the hybrid system will not reach the needed level [5] if the MPP is not monitored by a controller. Solar photovoltaic (PV) and wind turbine (Wind) power generating output voltages are well below the optimal operating level. As a result, a boost converter with an MPPT controller is used at each source to raise the output voltage to the necessary operating value of 220V. There is a lot of work to be done in the areas of grid integration and hybrid photovoltaic–wind power production. Multi-input hybrid PV–wind power generating system with a multi-input dc-dc converter and full-bridge dc–ac inverter has been suggested by Chen et al. [17], [7]. The dc-link voltage control is the primary goal of this system. Boost converters are used to match the dc-bus voltage from the outputs of a PV array and wind turbines in the six-arm converter architecture presented in [8]. Grid-connected hybrid PV and wind systems with battery storage are being studied in[9]. Among the topics covered here are energy generation, system dependability, and unit size, as well as costs and benefits analysis. Individual power converters are used to link a hybrid PV–wind system to a common dc-bus in [10], which also includes a battery. A separate inverter connects the dc-bus to the utility grid. There is rising interest in using multi-input converters for hybrid power systems because of their decreased component count, greater power density, compactness, and centralized control. For these reasons, other topologies have been proposed. They include non-isolated, completely isolated, and partly isolated multiport topologies. There are benefits to each of these.

Non-isolated multiport topologies have a shared ground for all of their power ports. Multiport dc-dc converters may be constructed using either a series or parallel input design [11–15]. Each input port may share several components.

The energy supply is constrained by the use of a time-sharing control method, which links each input port together. Multiport dc-dc converters may be derived from the series or parallel arrangement at the output [16]. It is not possible to share the power components, on the other hand. All non-isolated multiport topologies are generally combinations of the fundamental topology units, such as the buck, the boost, the buck-boost, or the bidirectional buck/boost topology unit. With these time-sharing multiport topologies, you may expect inexpensive installation costs and ease of use. However, a typical constraint is the inability to transmit power from several inputs to a load at the same time. These circuits will also have a tough time matching voltages over a broad range. Consequently, isolated multiport converters were preferred by researchers over non-isolated multiport dc-dc converters.

With two renewable power sources, the proposed system includes the grid and a battery. As a result, a power flow management system is necessary to ensure that all of these sources get equal amounts of electricity. The following are the system's primary goals. To investigate a multi-objective control strategy for optimum battery charging utilizing numerous sources. Uninterruptible power supply for loads making sure that excess power generated by renewable sources is sent to the grid and that the battery may be recharged by using the grid as and when necessary.

A hybrid distributed power generation system based on photovoltaics and batteries is shown in Figure 1. PV panels, ESS units (like batteries), and DC loads make up this three-part system. Balanced power flow is achieved in a PV/battery hybrid system by charging or draining the battery at the appropriate time. For example, as seen in Figure 1, the integrated bidirectional DC-to-DC converter and the bidirectional converter share the same power switches. Compared to conventional design, this boosts power density.

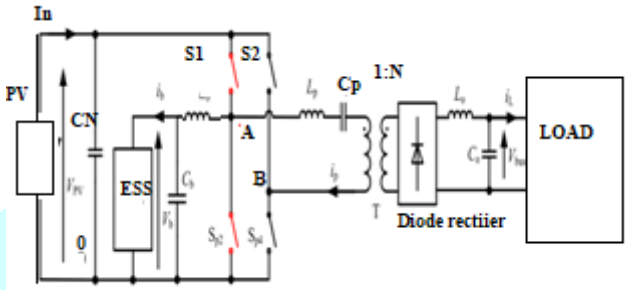

Figure 1: The proposed PV/battery hybrid distributed power generation system.

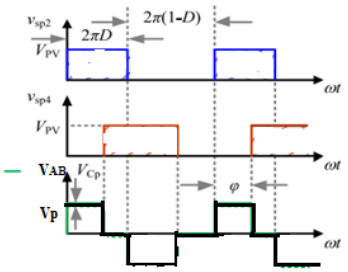

Figure 2: Modulation strategy of the full-bridge with the phase shift angle and the duty cycle D.

The principal complete bridge uses a modified phase-shift modulation method, as illustrated in Figure 2. The principal complete bridge's two switching legs are phase-shifted by an angle of Leg A switches S1 and S2 have a variable duty cycle, whereas the other two switches' duty cycles are set at 50%.

Figure 2 shows the battery-to-HF transformer bidirectional buck/boost converter incorporated into the main site of the transformer. Leg A's two power switches, the battery, capacitor Cb, inductor Lb, and the PV side bus all work together to provide an essentially bidirectional buck/boost architecture. The buck mode is activated when ib> 0 is charged to the battery. When the battery is completely drained, the topology switches to the "boost" mode. As a result, the battery's bidirectional power flow may be realized with the management's need for charging and discharging.

To accomplish maximum power point tracking (MPPT) in a buck/boost system, the PV output voltage may be managed by controlling the duty cycle D, as battery voltage Vb can be regarded as practically constant during normal SOC. If the inductor Lb is big enough, V_{PV} may be calculated as follows:

$$V_{PV} = V_b/K \quad (1)$$

K is the duty cycle of leg A's switch S1 as seen in Fig. 1. Another variable that may be used to regulate the DC bus voltage Vbus is the phase shift angle with two legs of the complete bridge modulated asymmetrically, VAB's DC component may affect the normal functioning of its HF transformer.

DC blocking capacitor Cp is used to prevent the HF transformer from overheating. The DC blocking capacitor Cp voltage VCp is obtained from the inductor Lp and HF transformer volt-second balancing concept as follows:

$$Vcp = Vpv\left(K - \frac{1}{2}\right) \quad (2)$$

Assuming the inductor Lo is large enough and using the volt-second balance principle, the DC bus voltage Vbus may be written as

$$V_{bus} = N\left\{\frac{\varphi}{2\pi}\left(V_{PV} - V_{Cp}\right) + \left(\frac{1}{2} + \frac{\varphi}{2\pi} - K\right)\left(V_{PV} + V_{Cp}\right) + \left[1 - \left(\frac{1}{2} + \frac{\varphi}{2\pi} - K + \frac{\varphi}{2\pi}\right)\right]\left|V_{Cp}\right|\right. \quad (3)$$

where 1:N is used to specify the transformer's turns ratio. The DC bus voltage Vbus can then be calculated as

$$V V_{bus} = \begin{cases} NV_{PV}\frac{\varphi}{\pi}\left[\frac{3}{2} - K\right] \\ NV_{PV}\left[\frac{\varphi}{\pi}\left(\frac{1}{2} + K\right) + \frac{1}{2} - 2K^2\right] \end{cases} \qquad K > \frac{1}{2},\ K > \frac{1}{2} \quad (4)$$

Fig. 3 shows that the modulation scheme must adhere to the following restrictions.

$$\begin{cases} K > \frac{\phi}{2\Pi} \\ \frac{1}{2} + \frac{\phi}{2\Pi} - K > 0 \end{cases} \quad (5)$$

A matched energy management and control strategy is given in the following section since and K are the only two control variables for the proposed PV/battery hybrid distributed power generation system.

$$\frac{\phi}{2\Pi} < \mathrm{K} < \frac{\phi}{2\Pi} + \frac{1}{2} \quad (6)$$

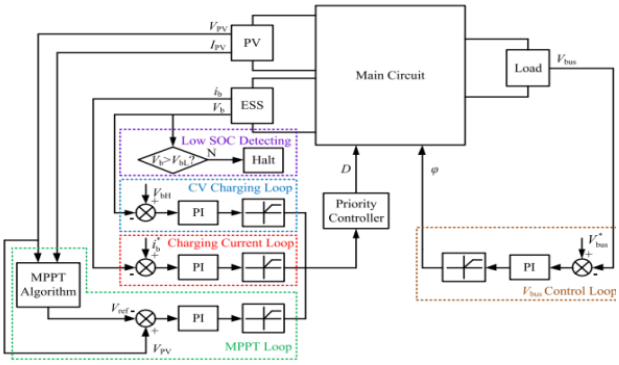

Figure 3. The control algorithm of the proposed PV/battery hybrid distributed power generation system.

II. CONTROL ALGORITHM

With this distributed PV/battery system, a control method is shown in Figure 3. [2] provides an explanation of MPPT methods. Since improving algorithms isn't the goal of this study, just incremental conductance MPPT is used. Figure 3 demonstrates how the phase shift angle of the bridge is utilised to adjust the voltage on the load side of the DC bus. Increasing conductance MPPT is used to create the PV reference voltage. In order to temporarily halt system function if battery voltage Vb falls below VbL, a low SOC detection element is added to the control system's architecture. In terms of power balance and automation, the most important system control variable is the duty cycle (K). MPPT control loops, CV charging, and charging current fight for duty cycle K. Control loops may be activated using this controller. Battery charging and discharging are made easier and more efficient when the PV is operating at its maximum capacity. Outputs from the priority controller are the lowest. While remaining within the PV and battery power range, when the load power PL exceeds PMPP's maximum output power. The charging current loop's output is saturated when ib becomes negative. It is activated when the battery voltage Vb is lower than that of the CV charging voltage VbH, and the duty cycle K is regulated until the PV works at or near its maximum power. Power is provided by the battery.

If the MPPT control loop is active, the solar panels may have additional power, resulting in excessive battery charging when demand is low. Due to the charging current control loop's input errors, the loop will charge over duty cycle K in this situation. The CV charging loop will be disabled if Vb is lower than VbH. The charging process would then switch to a constant current (CC) mode. Adjusting the PV's operating point and output voltage would be necessary to achieve power balance. The battery starts charging when Vb reaches the pre-set CV charging voltage VbH. Due to the erratic nature of CV charging, the PV operating point must be tweaked. The following is a list of possible scenarios for the proposed PV/battery hybrid distributed energy system under different power circumstances.

Scenario 1: The load power is greater than the maximum combined PV output and batteries. Unless the whole system is shut down, or steps like load shedding are adopted to alleviate the problem, this is the only option.

Scenario 2: The load power is greater than the PV's maximum output power (PMPP), but it is within the PV and battery's combined maximum power range. The MPPT control loop would be able to utilise the greatest quantity of solar energy conceivable in this condition. To keep the system's power balance, the battery would simultaneously drain some of its energy and provide some of it.

Scenario 3: The maximum power of the PV system is equal to the total power of the load. Batteries are never charged or discharged in this scenario, and instead, solar panels provide all of a home's energy needs.

Scenario 4: In this instance, the PV maximum power PMPP is greater than the load power, and the extra PV power is within the PV's maximum charging power for the battery. The MPPT control loop would be turned on in this case, enabling the PV to provide the load while also charging the battery. The battery serves as the system's power balance port in this situation.

Scenario 5: Under the particular irradiance and temperature circumstances, PMPP is more than total loads and battery charging power. In these circumstances. MPPT control loop would be disengaged and the battery charging current inthe control loop would be activated. If I b is predetermined, the battery will charge at a fixed pace in the constant current mode. However, until a power balance of the system is reached, the PV's operating point would be controlled appropriately. The battery's maximum discharge rate exceeds the load's maximum discharging rate.

Scenario 6: The photovoltaic output is approaching zero (for example in the evening). Either the whole system must be shut down, or measures like load shedding must be used.

Scenario 7: The battery's maximum discharge power is approaching zero and its PV output power is close to zero. As the only power source, the battery would be discharged in this scenario.

Table 1 provides a visual representation of the various operational situations outlined above. The battery's maximum discharging and charging power denoted as P_{Max} DCHG and P_{Max} CHG, are both governed by the battery's unique application needs. Also shown in Fig. 4 is a flow diagram of the suggested controller algorithm.

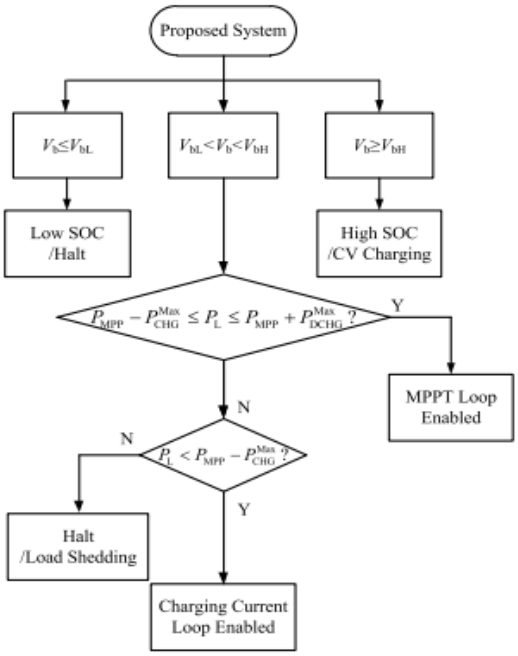

Figure 4. Flow diagram of the proposed control algorithm.

Table 1. Operation scenarios of the system.

Scenarios	Power Conditions	MPPT
1	$\boldsymbol{P_L > P_{MPP} + P_{DCHG}^{Max}}$	-
2	$\boldsymbol{P_{MPP} \le P_{MPP} + P_{DCHG}^{Max}}$	Enabled
3	$\boldsymbol{P_L - P_{MPP}}$	Enabled
4	$\boldsymbol{P_{MPP} - P_{CHG}^{Max} \le P_L < P_{MPP}}$	Enabled
5	$\boldsymbol{P_L < P_{MPP} - P_{CHG}^{Max}}$	-
6	$\boldsymbol{P_{pv} = 0, P_L > P_{DCHG}^{Max}}$	-
7	$\boldsymbol{P_{pv} = 0, P_L > P_{DCHG}^{Max}}$	-

III. INDUCTION MOTOR

An induction motor whose rotor current is induced by the stator's magnetic field. Induction motor rotors aren't connected like universal, DC, and synchronous motors. Analog asynchronous motors employ wound or squirrel-cage rotors.

3ϕ squirrel-cage asynchronous motors are durable, reliable, and economical. Ceiling fans use single-phase induction motors. Induction motors are increasingly used with variable-frequency drives (VFDs) in variable-speed operation. Induction motors may save energy with variable-torque centrifugal fan, pump, and compressor loads. Squirrel cage induction motors are widely used in fixed-speed and VFD applications. Variable-speed applications use variable-voltage and variable-frequency drivers.

AC power delivered to the stator of induction and synchronous motors spins a magnetic field. A synchronous motor's rotor spins at the same speed as the stator field, whereas an induction motor's rotor spins slower. The rotor's magnetic field orbits the stator's. Short-circuiting or closing the external impedance causes an opposing current to flow in the induction motor's secondary winding. Revolving magnetic flux windings create currents like transformer secondary windings (s). The rotor's winding current creates magnetic fields. Lenz's Law says the magnetic field will point in the opposite direction of the rotor's current. Due to the revolving stator's influence on winding-induced current, the spinning rotor starts to rotate in the direction of that magnetic field. Until the applied load equals the induced rotor current and torque, the rotor accelerates. Induction motors never operate synchronously because there is no induced rotor current. The "slip" between actual and synchronous speed for Design B induction motors is 0.5 to 5%. Induction machines are created entirely by induction, unlike synchronous, DC, or permanent magnet motors.

To generate rotor currents, the rotor's physical speed must be lower than the stator's spinning magnetic field's (ns) speed; otherwise, the magnetic field wouldn't move relative to the rotor conductors and no currents would be formed. When the spinning magnetic field slows, more current flows through the windings and torque is created. Slip is the difference between the rotor's induced magnetic field and the stator's rotating field. Slip increases torque when speed and load are reduced. Induction motors are also called "asynchronous motors." An induction motor may be employed as a generator or unrolled to provide linear motion.

Synchronous Speed:

Synchronous speed refers to the magnetic field's rotational speed.

$$\frac{120 \times F}{P} \qquad (7)$$

Where, F = supply frequency

P = no. of poles

The rotor spins synchronously with the stator field. Rotor is always behind. If the rotor speed catches up to the stator speed, no induced rotor current or torque is needed to keep the rotor spinning. The rotor will slow due to diminished torque, but the motor will continue to operate due to relative speed. Consequently, rotor speed is lower than synchronous speed. Slip is the difference between Ns and the rotor's actual speed (N).

$$\% \text{ slip } S = \frac{Ns - N}{Ns} \times 100 \qquad (8)$$

Microgrid

As the electric distribution industry enters the twenty-first century, many developments are emerging that will alter the way energy is delivered. Demand for these changes is being driven by the need for increased energy availability and efficiency, while supply is being pushed by the need to accommodate distributed generation and peak-having technology.

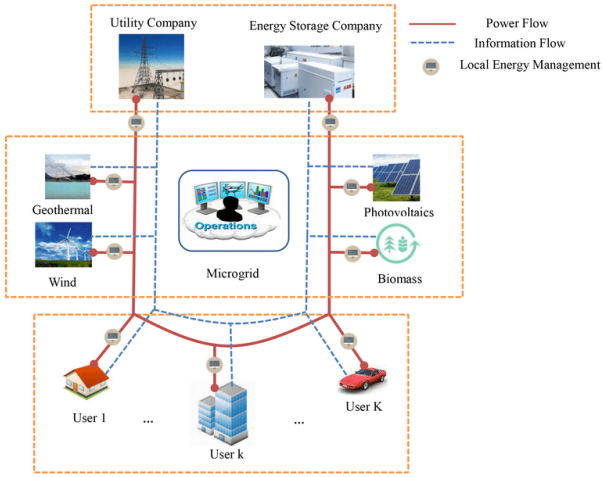

Figure 5.Microgrid power system

As deregulation and dispersed energy supplies rise, power systems' operating demands are changing (DER). Many DERs employ RES such as solar, wind, and hydropower for small-scale generating (micro sources). Microsources near the load minimise transmission losses and network congestion. In the case of severe system outages, surrounding micro sources, regulated loads, and energy storage systems may run in islanded mode, lowering the likelihood of end-customer power interruptions. We have a microgrid. Figure 5 shows a conventional microgrid. The 1 MVA microgrid is the same size as low-voltage distribution feeders. Over 90% of low-voltage house customers are serviced via underground cable, the rest by overhead lines. The microgrid may deliver power and heat to homes and businesses using CHPs, gas turbines, fuel cells, PV systems, and wind turbines. Batteries and flywheels store energy. A microgrid energy storage device functions as a rotating reserve for typical grid generators, balancing energy output and consumption during demand or generation oscillations.

Microgrids distribute thermal and electrical energy to clients, enhancing local dependability, reducing emissions, boosting voltage support, and perhaps lowering energy supply costs. Distributed energy sources may reduce utilities' transmission and distribution needs. Distributed generation near loads reduces transmission and distribution circuit flows, reducing loss and perhaps replacing network assets. A close-to-demand generation may boost customer satisfaction. Microgrids reduce congestion and speed up network recovery when the network is stressed. Microgrids may reduce GHG emissions and mitigate climate change. Distributed generating units use renewable and low-emission microsources.

Microgrids may boost energy efficiency, reduce total energy consumption, reduce greenhouse gas emissions and other pollutants, improve service quality, and reduce costs when replacing current electrical infrastructure.

Microgrids provide several technological challenges. To provide steady operation during network disruptions, stability, and power quality in islanding mode, micro grid inverters need more advanced control algorithms. These reasons have attracted researchers and government agencies in the U.S., Europe, and Japan about microgrids. Microgrid integration and operation present various technical obstacles.

IV. SIMULATION RESULTS:

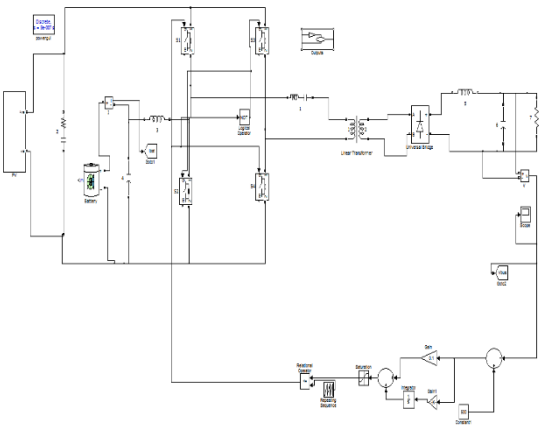

Figure 6 Diagram of Proposed System

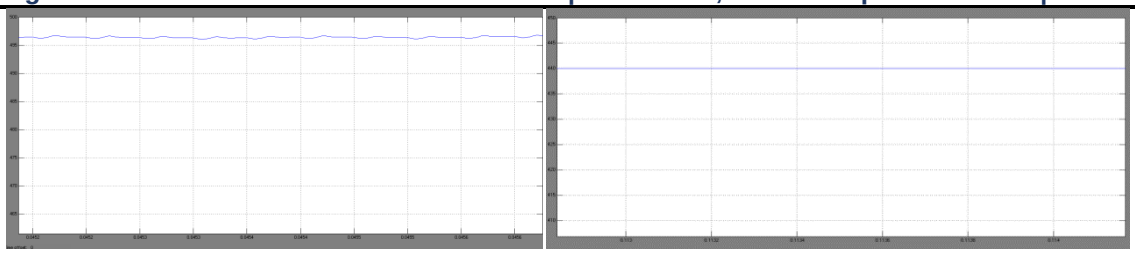

(a) (b)

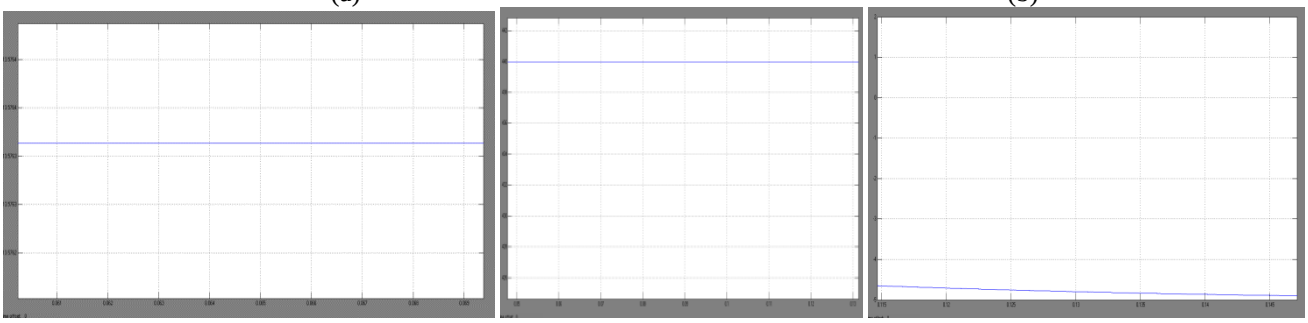

(c) (d) (e)

Figure 7 Simulation results of operation scenario 2. (a) DC bus voltage Vbus; (b) PV voltage VPV; (c) PV current IPV; (d) PV reference voltage Vref; (e) Batter charging current ib.

Figure 7 shows steady-state simulation findings. Simulation parameters: 1000 W/m2 of sunshine, 25 C. Fig. 7 shows how a PI controller manages the phase shift angle to maintain Vbus D 500 V. (a). As illustrated in Fig. 7(b), (c), and 7(d), when the MPPT loop is initiated, the PV operates near VMPP D 435 V and the IPV near IMPP D 22 A at its maximum power point. In discharging mode, the battery supplies some of the load's power (Fig. 7). (e).

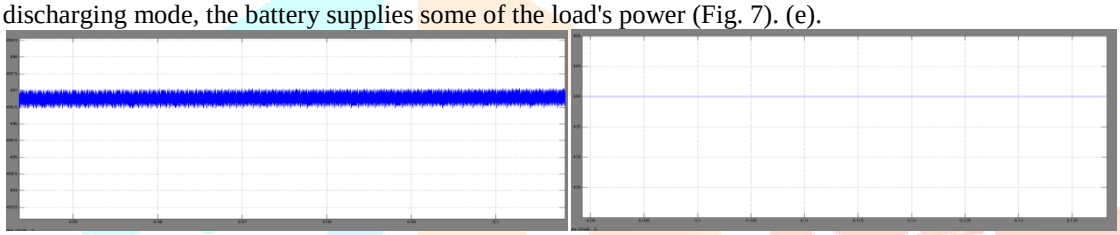

(a) (b)

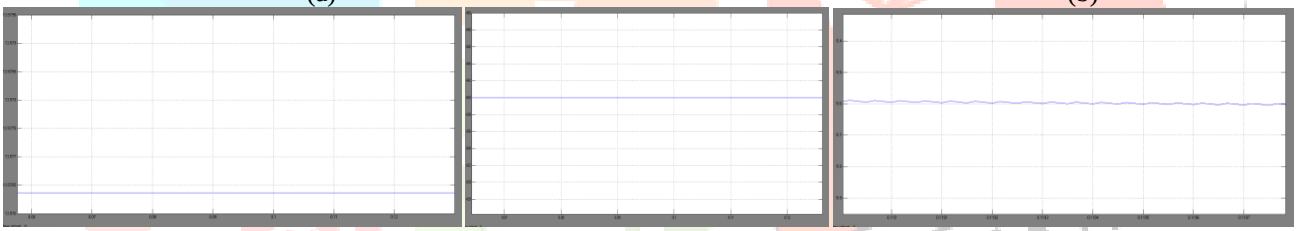

(c) (d) (e)

Figure 8. Simulation results of operation scenario 4. (a) DC bus voltage Vbus; (b) PV voltage VPV; (c) PV current IPV; (d) PV reference voltage Vref; (e) Battery charging current ib.

Figure 8 shows steady-state simulation results. Simulation parameters: PL D 8 kW at 1000 W/m2 and 25°C. As seen in Fig. 8, the DC bus voltage Vbus is 500 V. (a). Fig. 8 (b) indicates that the MPPT loop is triggered and the PV operates at maximum power point with VPV around VMPP D 435 V and IPV around IMPP D 22 A, which is close to the ideal VMPP D 435 V. Fig. 8(e) demonstrates that the battery is in charging mode and can store extra PV power.

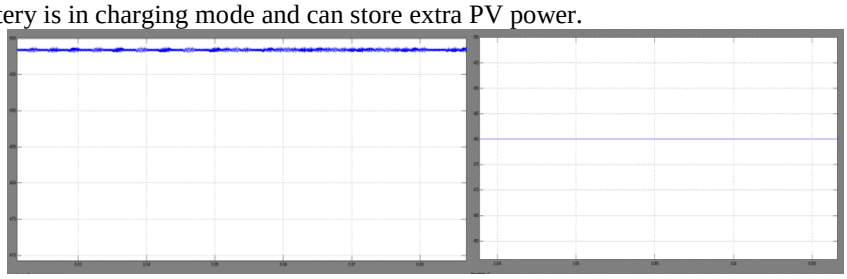

(a) (b)

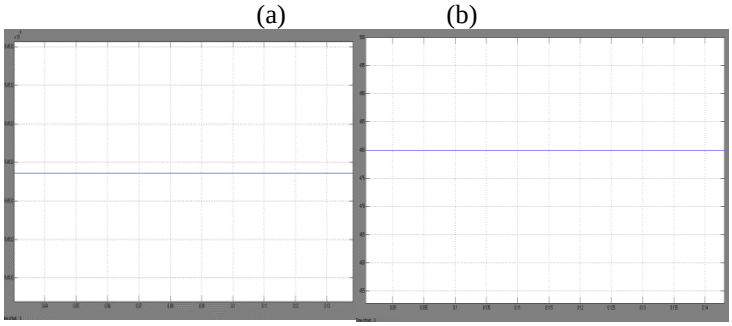

(c) (d)

FIGURE 9 Simulation results of operation scenario 5. (a) DC bus voltage Vbus; (b) PV voltage VPV; (c) PV current IPV; (d) Battery charging current ib

Senario5 Simulated Stability Figure 9 displays results. Simulation parameters: 25°C, 2:5kW, 1000W/m2 Figure 9 illustrates that Vbus is controlled at 500 Vbus D. (a). Figure 9 illustrates I b D 30 A, the battery charging current controlled by the maximum charging current loop and the MPPT loop (d). Figures 9 (b) and (c) indicate that the PV would not operate at its maximum power point to preserve power balance.

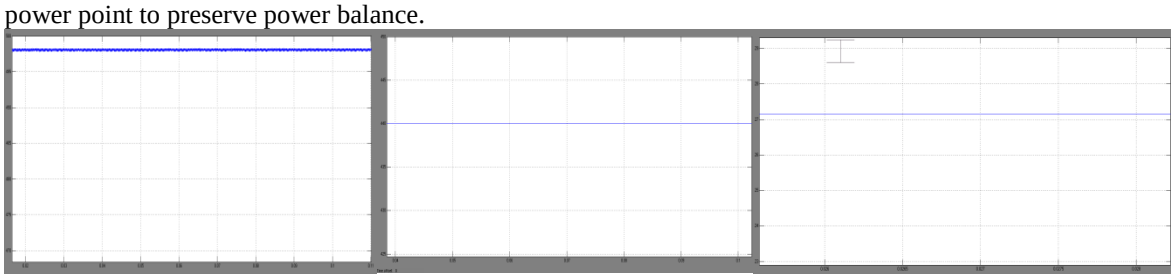

(a) (b) (c)

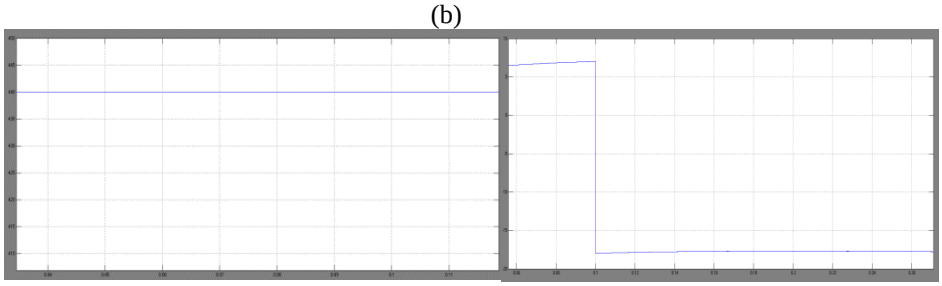

(d) (e)

Figure10. Simulation results with irradiance dropping from 1000 W/m2 to 500 W/m2 at t D 2 s. (a) DC bus voltage Vbus; (b) PV voltage VPV; (c) PV current IPV; (d) PV reference voltage Vref; (e) Battery charging current ib.

Figure 10 demonstrates that when irradiance drops from 1000 to 500 W/m2, the system runs at t D2 s. 8 kW PL, 25°C; D 25°C. FIGURE 10: DC bus voltage change (a). Here, MPPT regulates D. Because the PV curve changes, Vref rises (Figure 10). (d). The PV must be near its MPP in Figure. 10 (b) and (c) to monitor maximum power point (c). Figure 10(e) demonstrates a transition from scenario 4 (charging battery) to scenario 2 (discharging battery).

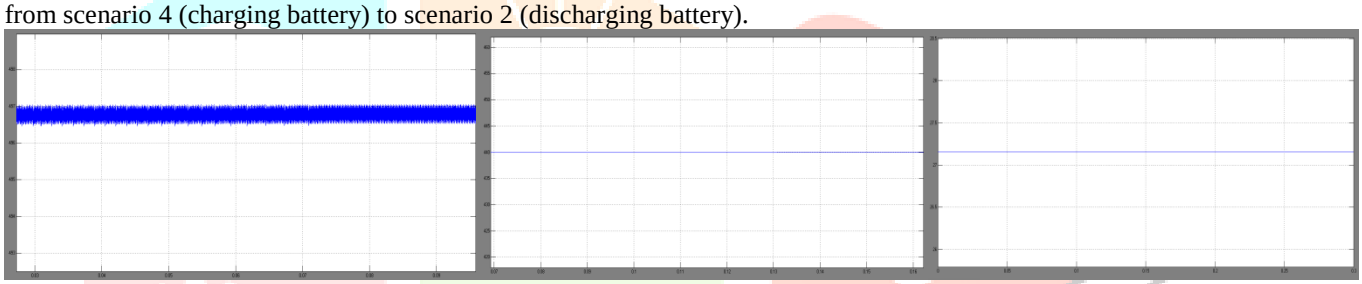

(a) (b) (c)

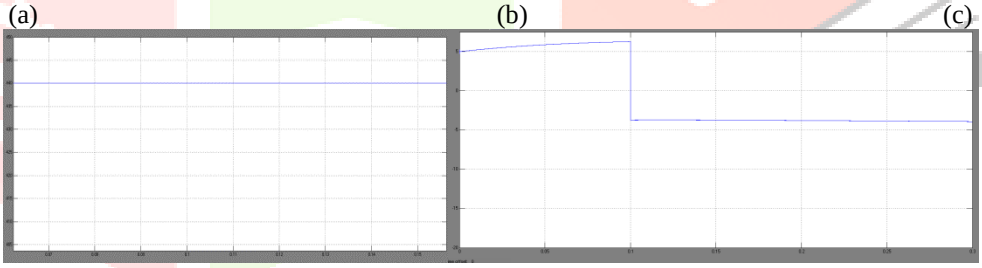

(d) (e)

FIGURE 11. Simulation results with load power rising from 8 kW to 10 kW at t D 2 s. (a) DC bus voltage Vbus; (b) PV voltage VPV; (c) PV current IPV; (d) PV reference voltage Vref; (e) Battery charging current ib.

Figure 11 shows the system's dynamic performance when PL grows from 8 kW to 10 kW in two seconds. Simulator settings include: 25C, 1000W/m2 Fig. 11 illustrates that Vbus stays constant throughout the shift (a). Figures 11(b) through 11(c) show that the MPPT loop is constantly active (d). This increase in load power shifts from mode 4 to mode 2 (Figure 11). (e).

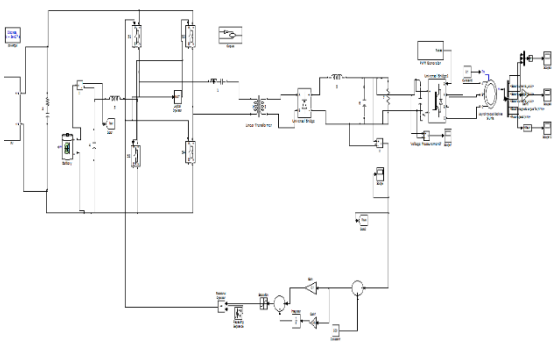

Figure 12 Simulink diagram of a Proposed System power converter with Induction Motor drive

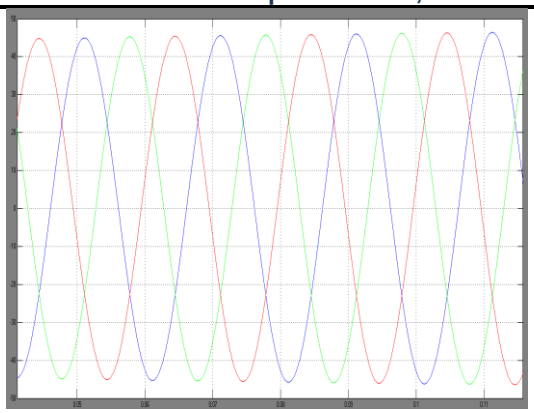

Figure 13 Simulation waveforms of Induction motor drive stator current characteristics

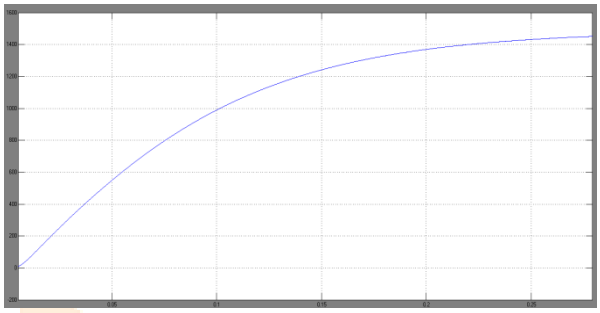

Figure 14 Simulation waveforms of Induction motor drive speed characteristics

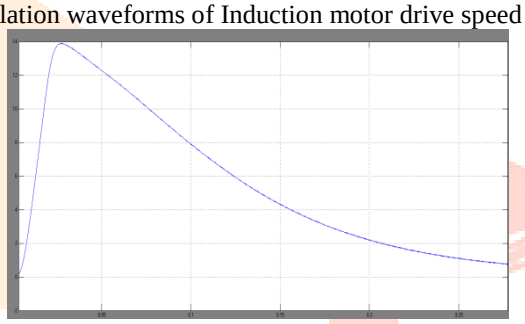

Figure 15 Simulation waveforms of Induction motor drive Torque characteristics

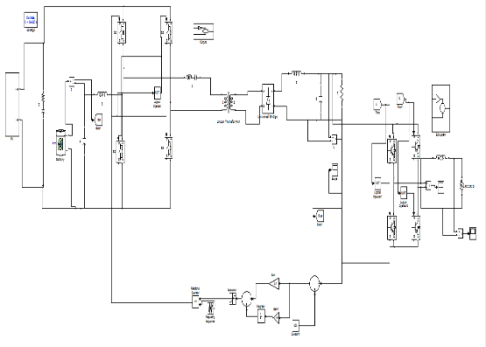

Figure 16 Simulink diagram of a Proposed System power converter with Grid-connected Systems

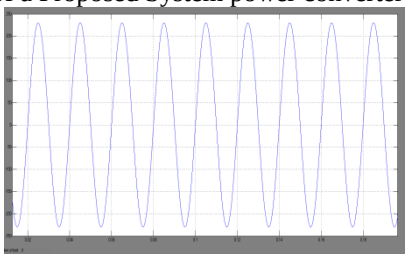

Figure 17 Simulation waveforms of Grid-connected proposed system characteristics

V. CONCLUSION

A three-port integrated power converter with induction motor drive and grid applications is recommended for the PV/battery hybrid distributed power generation system. The recommended Induction motor drive and grid system has two advantages over a standard DC-DC unidirectional conversion stage and a bidirectional conversion stage: higher power density and dependability. Control variables include the complete bridge phase shift angle and the switch duty cycle to achieve the desired DC bus voltage and to distribute power evenly across the three ports. An energy management and control plan is suggested based on a thorough examination of the system's numerous operating situations. Depending on the situation, the priority controller may activate one of the control loops to improve overall system performance while also making use of MPPT and managing battery charging and discharge. The results of the simulation show that the suggested induction motor drive and grid applications PV/battery hybrid distributed power generating system function as expected and that the control method is feasible.

REFERENCES

[1] J. Hong, J. Yin, Y. Liu, J. Peng and H. Jiang, "Energy Management and Control Strategy of Photovoltaic/Battery Hybrid Distributed Power Generation Systems With an Integrated Three-Port Power Converter," in IEEE Access, vol. 7, pp. 82838-82847, 2019, doi: 10.1109/ACCESS.2019.2923458.

[2] T. Esram and P. L. Chapman, ''Comparison of photovoltaic array maximum power point tracking techniques,'' IEEE Trans. Energy Convers., vol. 22, no. 2, pp. 439–449, Jun. 2007.

[3] J. M. Carrasco, L. G. Franquelo, J. T. Bialasiewicz, E. Galvan, R. Potillo, M. M. Prats, J. I. Leon, and N. Moreno-Alfonso, ''Power-electronic systems for the grid integration of renewable energy sources: A survey,'' IEEE Trans. Ind. Electron., vol. 53, no. 4, pp. 1002–1016, Jun. 2006.

[4] BP Statistical Review of World Energy, British Petroleum, London, U.K., Jun. 2018.

[5] J. P. Barton and D. G. Infield, ''Energy storage and its use with intermittent renewable energy,'' IEEE Trans. Energy Convers., vol. 19, no. 2, pp. 441–448, Jun. 2004.

[6] W. Li, J. Xiao, Y. Zhao, and X. He, ''PWM plus phase angle shift (PPAS) control scheme for combined multiport DC/DC converters,'' IEEE Trans. Power

[7] C. A. Hill, M. C. Such, D. Chen, J. Gonzalez, and W. M. Grady, ''Battery energy storage for enabling integration of distributed solar power generation,'' IEEE Trans. Smart Grid, vol. 3, no. 2, pp. 850–857, Jun. 2012.

[8] Z. Yi, W. Dong, and A. H. Etemadi, ''A unified control and power management scheme for PV-battery-based hybrid microgrids for both gridconnected and islanded modes,'' IEEE Trans. Smart Grid, vol. 9, no. 6, pp. 5975–5985, Nov. 2018.

[9] H. Mahmood, D. Michaelson, and J. Jiang, ''Decentralized power management of a PV/battery hybrid unit in a droop-controlled islanded microgrid,'' IEEE Trans. Power Electron., vol. 30, no. 12, pp. 7215–7229, Dec. 2015.

[10] K. Sun, L. Zhang, Y. Xing, and J. M. Guerrero, ''A distributed control strategy based on DC bus signaling for modular photovoltaic generation systems with battery energy storage,'' IEEE Trans. Power Electron., vol. 26, no. 10, pp. 3032–3045, Oct. 2011.

[11] S. Adhikari and F. Li, ''Coordinated V-f and P-Q control of solar photovoltaic generators with MPPT and battery storage in microgrids,'' IEEE Trans. Smart Grid, vol. 5, no. 3, pp. 1270–1281, May 2014.

[12] S. K. Kollimalla, M. K. Mishra, and N. L. Narasamma, ''Design and analysis of novel control strategy for battery and supercapacitor storage system,'' IEEE Trans. Sustain. Energy, vol. 5, no. 4, pp. 1137–1144, Oct. 2014.

[13] S. Wen, S. Wang, G. Liu, and R. Liu, ''Energy management and coordinated control strategy of PV/HESS AC microgrid during Islanded operation,'' IEEE Access, vol. 7, pp. 4432–4441, 2019.

[14] W. Jiang and B. Fahimi, ''Multiport power electronic interface—Concept, modeling, and design,'' IEEE Trans. Power Electron., vol. 26, no. 7, pp. 1890–1900, Jul. 2011.

[15] H. Krishnaswami and N. Mohan, ''Three-port series-resonant DC–DC converter to interface renewable energy sources with bidirectional load and energy storage ports,'' IEEE Trans. Power Electron., vol. 24, no. 10, pp. 2289–2297, Oct. 2009.

[16] H. Tao, J. L. Duarte, and M. A. M. Hendrix, ''Three-port triple-half-bridge bidirectional converter with zero-voltage switching,'' IEEE Trans. Power Electron., vol. 23, no. 2, pp. 782–792, Mar. 2008.

[17] M. S. Whittingham, ''History, evolution, and future status of energy storage,'' Proc. IEEE, vol. 100, pp. 1518–1534, May 2012.

[18] F. Blaabjerg, Z. Chen, and S. B. Kjaer, ''Power electronics as efficient interface in dispersed power generation systems,'' IEEE Trans. Power Electron., vol. 19, no. 5, pp. 1184–1194, Sep. 2004.